An aerobic link between lignin degradation and C_1 metabolism: growth on methoxylated aromatic compounds by members of the genus *Methylobacterium*

Jessica A. Lee[12345], Sergey Stolyar[123], and Christopher J. Marx[123]

Running title

Methylobacterium growth on methoxylated aromatics

Affiliations

[1]Department of Biological Sciences, University of Idaho, Moscow, ID

[2]Center for Modeling Complex Interactions, University of Idaho, Moscow, ID

[3]Institute for Bioinformatics and Evolutionary Studies, University of Idaho, Moscow, ID

[4]Global Viral, San Francisco, CA

[5]Department of Biology, San Francisco State University, San Francisco, CA

Corresponding authors

Jessica A. Lee: jessica.audrey.lee@gmail.com

Christopher J. Marx: cmarx@uidaho.edu

Abstract

Microorganisms faces many barriers in the degradation of the polycyclic aromatic polymer lignin, one of which is an abundance of methoxy substituents. Demethoxylation of lignin-derived aromatic monomers in aerobic environments releases formaldehyde, a potent cellular toxin that organisms must eliminate in order to further degrade the aromatic ring. Here we provide the first comprehensive description of the ecology and evolution of the catabolism of methoxylated aromatics in the genus *Methylobacterium*, a plant-associated genus of methylotrophs capable of using formaldehyde for growth. Using comparative genomics, we found that the capacity for aromatic catabolism is ancestral to two clades, but has also been acquired horizontally by other members of the genus. Through laboratory growth assays, we demonstrated that several *Methylobacterium* strains can grow on *p*-hydroxybenzoate, protocatechuate, vanillate, and ferulate; furthermore, whereas non-methylotrophs excrete formaldehyde as a byproduct during growth on vanillate, *Methylobacterium* do not. Finally, we surveyed published metagenome data to find that vanillate-degrading *Methylobacterium* can be found in many soil and rhizosphere ecosystems but is disproportionately prominent in the phyllosphere, and the most highly represented clade in the environment (the root-nodulating species *M. nodulans*) is one with few cultured representatives.

Introduction

Microbial processes for degrading lignin and lignin-derived aromatics are of intense interest in a diversity of fields, ranging from bioenergy engineering—in which the recalcitrance of lignin is a major hurdle in the processing of plant biomass [1]—to the fossil fuel industry—which seeks to understand microbial transformations of coal [2]. Lignin, which comprises approximately 20% of the carbon fixed by photosynthesis on land [3], is an exceptionally complex, irregular, polycyclic aromatic polymer, in which many of the constituent aromatic rings are heavily substituted with methoxy ($-OCH_3$) groups [4].

In the aerobic microbial degradation of lignin-derived aromatic monomers such as vanillate, the degradation of the aromatic ring proceeds by the protocatechuate branch of the beta-ketoadipate pathway. The gene cluster encoding this pathway is widely distributed among soil microorganisms, and has a complex evolutionary history resulting in diverse patterns of gene organization and regulation [5–7]. In the case of methoxylated aromatics, ring cleavage must be preceded by the removal of the methoxy group; in most aerobic organisms, this occurs via vanillate monooxygenase, a Rieske [2Fe-2S] enzyme that demethylates vanillate to generate protocatechuate and formaldehyde [8–12] (Fig. 1). Formaldehyde is a potent electrophile, and toxic to microorganisms due to its reactivity with DNA and proteins [13]. Elimination of this toxin is therefore essential to lignin degradation. Multiple studies have demonstrated experimentally, through either engineered disruption or constitutive expression of formaldehyde oxidation capacity in *Bradyrhizobium diazoefficiens* [11], *Pseudomonas putida* [14], *Burkholderia cepacia* [9], and *Corynebacterium glutamicum* [15], that demethoxylation of vanillate is dependent on the activity of an functional formaldehyde detoxification system, and formaldehyde removal may be the rate-limiting step to the degradation of lignin-derived methoxylated aromatics.

Detoxification pathways in lignin-degrading organisms are diverse, and in some organisms include more than one mechanism. In some cases formaldehyde is oxidized

to CO_2 via formate, such as in the thiol-dependent systems in *C. glutamicum* and *B. japonicum* or the zinc-dependent dehydrogenase in *P. putida* [16]; in others it may be incorporated into biomass via the RuMP pathway, as in *B. cepacia* [17]. Furthermore, it has recently been discovered that methanogens of the genus *Methermicoccus* are capable of using the methoxy groups of coal-derived aromatic compounds for the production of methane through a novel metabolic pathway ("methoxydotrophic methanogenesis"), illuminating a previously-unknown link between coal degradation and methane production via C_1 metabolism [18].

Methylotrophs, organisms that use reduced C_1 compounds for growth, therefore make appealing candidates for efficient degradation of lignin-derived methyoxylated aromatics. Members of the genus *Methylobacterium*, and particularly the model organism *M. extorquens*, have long been studied for their metabolism of simple C_1 compounds such as methanol, formate, methylamine, and halogenated methanes [19]. Formaldehyde is a central intermediate in the metabolism of many of these substrates, raising the possibility that, if *Methylobacterium* were capable of demethoxylating aromatic compounds, they could also use the resulting formaldehyde as a growth substrate. It has previously been documented that two members of the genus are capable of growth on aromatic compounds [20–22]; however, the prevalence of this trait among *Methylobacterium* and the organization and evolutionary history of the genes involved has not been described. Furthermore, to our knowledge, it has not been shown whether these organisms are capable of methoxydotrophy: growth on methoxy groups from aromatic compounds.

Here we report novel findings on the ecology and evolution of methoxydotrophic growth and catabolism of aromatic compounds by members of the genus *Methylobacterium*. We explored the genomic capacity of *Methylobacterium* species by searching published genomes, verified growth and formaldehyde production/consumption on aromatic compounds in the laboratory, and surveyed published metagenome data to assess the distribution and prevalence of aromatic-degrading *Methylobacterium* in the environment. For a thorough description of aerobic microbial degradation of lignin-derived aromatic

101 compounds, we direct the reader to the excellent reviews published previously [5, 23]; a
102 simplified diagram of the pathway and the four genes of interest to this study (*vanA*,
103 *pcaG*, *pobA*, *ech*) is given in Figure 1. Because we were especially interested in
104 organisms that could use the methoxy group of vanillate, our metagenomic analysis
105 focused especially on *vanA* (KO:K03862), the gene encoding the alpha subunit of
106 vanillate monooxygenase.
107
108
109 **Materials and Methods**
110
111 **Phylogenetic analysis**
112 Genetic potential of *Methylobacterium* species [24] (Table S1) for the degradation of
113 aromatic compounds was assessed through analysis of genomes available on the
114 IMG/M database [25]. We should note that Green and Ardley [26] recently proposed a
115 restructuring of the genus *Methylobacterium*, including a renaming of the genus of the
116 *M. extorquens* clade from *Methylobacterium* to *Methylorubrum*, and a suggestion to
117 reclassify the *M. aquaticum* and *M. nodulans* clades into different genera entirely.
118 However, because the present study is concerned with the four clades as a coherent
119 group of evolutionarily related taxa that are still known as *Methylobacterium* by many
120 research groups, and all are currently still listed within that genus by the List of
121 Prokaryotic Names with Standing in Nomenclature [27], in this manuscript we continue
122 to refer to all organisms as *Methylobacterium*.
123
124 Genes of interest were identified by KEGG Orthology ID: *vanA* (vanillate
125 monooxygenase alpha subunit, KO:K03862); *pcaG* (protocatechuate 3,4-dioxygenase
126 alpha subunit, KO:K00448); *pobA* (*p*-hydroxybenzoate 3-monooxygenase, KO:K00481);
127 and *ech* (*trans*-feruloyl-CoA hydratase/vanillin synthase, KO:K18383; we searched also
128 for IMG Term Object ID 8865, vanillin synthase). Known lignin-degrading organisms
129 were added to the phylogenies as reference organisms, and *Prochlorococcus marinus*
130 NATL2A and archaeal species were used as outgroups (Table S2). The genes used for
131 the phylogeny in Figure 1 were 16S rRNA (the RNA component of the small ribosomal

132 subunit), *rpoB* (DNA-directed RNA polymerase subunit beta, KO:K03043), *atpD* (ATP
133 Synthase F1 complex beta subunit, KO:K02112), and *recA* (recombination protein
134 RecA, KO:K03553), all of which have been shown previously to be informative for
135 phylogenetic analysis in *Methylobacterium* and closely related organisms [28–30].
136
137 All gene sequences were aligned using Clustal Omega v.1.2.3 [31], using four combined
138 HMM/guide tree iterations and default settings for all other parameters. Phylogenetic
139 trees were generated using IQ-Tree v.1.6.1 [32] on the CIPRES Science Gateway [33],
140 with one partition, outgroups given in Table S2, ultrafast bootstrapping with 1000
141 replicates, and SH-like Single Branch test [34] with 1000 replicates; for all other
142 parameters, the default settings were used.
143
144 **Genomic context of aromatic catabolism genes**
145 To assess synteny in the gene neighborhoods surrounding the *vanA* and *pcaH* genes in
146 *Methylobacterium* species, we aligned scaffolds, or segments of assembled genomes,
147 using MAUVE v.2.4.0 with the progressiveMauve algorithm and default parameter
148 settings [35, 36]. Figures were generated using a GenoPlotR v.0.8.7 [37] for R v.3.4.3
149 [38] in RStudio v.1.1.423 [39].
150
151 GC content in the *Methylobacterium sp*. AMS5 genome was calculated in R using the
152 alphabetFrequency function from Biostrings v.2.46.0 [40]; for the plot in Fig. S1, a
153 sliding window of 5 kb was used for the full genome and 500 bp for the catabolic island
154 region. Genome signature difference was calculated using a custom script in R, using
155 the formula for the δ* difference [41] with tetranucleotides rather than dinucleotides.
156
157 **Growth assays on aromatic substrates**
158 All organisms were grown on MPIPES medium [42] with the addition of 1x Wolfe's
159 Vitamins [43], 25 μM $LaCl_3$ (as has been found to facilitate growth in some
160 *Methylobacterium spp*. [44]), and carbon substrates as specified. All conditions
161 contained 16 mM of carbon (4 mM succinate, 2.67 mM glucose, 2.29 mM benzoate,
162 2.29 mM PHBA, 2.29 mM PCA, 2 mM vanillate, 1.6 mM ferulate, 0.4 g/L Kraft lignin).

163 *Methylobacterium* sp. 4-46 was also tested on methanol without $LaCl_3$. For each assay,
164 one colony was inoculated from a culture plate into 5 mL MPIPES with 3.5 mM disodium
165 succinate and grown 24 hours to obtain a stationary-phase culture, then diluted 1:64,
166 and grown again until stationary. Using that inoculum, the growth experiment was
167 conducted as follows: each replicate was diluted 1:64 into MPIPES and aliquoted into
168 several wells of a Costar 48-well tissue culture-treated plate (product #3548, Corning
169 Inc., Corning, NY) for non-volatile substrates, or into Balch-type glass culture tubes for
170 vanillin, along with carbon substrate provided at concentrations such that all conditions
171 were equimolar in carbon (16 mM). Total volume was 640 μL per well in culture plates
172 or 5 mL per tube in Balch tubes. Each strain was tested in biological triplicate (3
173 separate colonies). Balch tubes were sealed with butyl rubber serum stoppers to
174 prevent escape of vanillin.
175
176 Plates were incubated at 30 °C in a LPX44 Plate Hotel (LiCONiC, Woburn, MA) with
177 shaking at 250 RPM. Optical density was assessed using a Wallac 1420 Victor2
178 Microplate Reader (Perkin Elmer, Waltham, MA), reading OD_{600} for 0.4 seconds at
179 intervals of between 2 and 5 hours. Culture tubes were incubated in a TC-7 tissue
180 culture roller drum (New Brunswick Scientific, Edison, NJ) at a speed setting of 7, and
181 OD_{600} was measured in the culture tubes using a Spectronic 200 spectrophotometer
182 (Thermo Fisher Scientific, Waltham, MA). Outputs from the Wallac 1420 software were
183 collated using Curve Fitter [42]; data cleaning, analysis, and plotting were then
184 conducted using custom scripts in R (Supplemental Files S1, S2). Because many of the
185 strains formed clumps, maximum OD_{600} was used as a semi-quantitative metric for
186 growth. Non-growth was defined as no OD_{600} above 0.025.
187
188 **Formaldehyde production during growth on vanillate**
189 Growth of *Methylobacterium* strains on vanillate was initiated with stationary-phase
190 MPIPES-succinate cultures as described above; these were diluted 1:64 into 5 mL
191 MPIPES with 2 mM vanillate and grown 2 days until stationary phase. This inoculum
192 was diluted 1:32 into culture flasks containing 20 mL of MPIPES with 2 mM vanillate and
193 incubated, shaking, at 30 °C. Cultures were sampled every 4 hours: OD_{600} was

194 measured in a SmartSpec Plus Spectrophotometer (Bio-Rad Laboratories, Hercules,
195 CA), and the supernatant of 500 µL of centrifuged culture was used for the
196 measurement of formaldehyde using a colorimetric assay [45]. All strains were tested in
197 biological triplicate.
198
199 Formaldehyde production of non-methylotrophs during vanillate growth was assayed
200 similarly. Stationary-phase vanillate-grown cultures of *Pseudomonas putida* KT2440 and
201 *Rhodococcus jostii* RHA1 were diluted 1:64 into 5 mL MPIPES medium in culture tubes,
202 with sampling every 2 hours. Vanillate was provided at 4 mM; although this was greater
203 than in the *Methylobacterium* experiment, we have found that vanillate concentration
204 has little effect on the resulting concentration of formaldehyde in the medium (Fig. S3).
205
206 **Analysis of *Methylobacterium vanA* genes in published metagenomes**
207 To assess the abundance of *Methylobacterium*-encoded *vanA* genes in the
208 environment, we searched all published metagenomes available through the IMG/M
209 portal on December 20, 2017. The "Function Search" tool was used to identify all
210 metagenomes containing genes annotated with KO:K03862 (*vanA*). To increase our
211 chances of observing meaningful ecological patterns, we restricted our analysis
212 metagenomes containing >100 *vanA* genes. Genes on scaffolds with a phylogenetic
213 lineage assignment of *Methylobacterium* were designated "*Methylobacterium vanA.*"
214 and the ecological context was taken from the Ecosystem Type field in the sample
215 metadata associated with each gene. Because it was unclear whether all researchers
216 used consistent definitions, we combined phylloplane with phyllosphere, and rhizoplane
217 with rhizosphere.
218
219 To provide a tree-based assessment of *vanA* diversity in addition to the USEARCH-
220 based IMG/M phylogenetic lineage assignment [46], we downloaded the
221 *Methylobacterium vanA* gene sequences and placed them in the reference *vanA*
222 phylogeny (described above). Pplacer v.1.1 [47] was used with HMMer v.3.1b.2 [48],
223 RAxML v.8.2 [49], and taxtastic v.0.8.8 for Python 3. The resulting tree was paired with
224 metadata from sequence scaffolds in Phyloseq v.1.22.3 for R [50], to generate the plot

225 in Fig. 8.
226
227 The relative abundances of all *vanA* or all *Methylobacterium* reads within each
228 metagenome were found using the Statistical Analysis tool in IMG [25]. For each
229 Ecosystem Type, the average and standard error among metagenomes was calculated
230 manually, in order to omit datasets with "NA" values due to unassembled genes that
231 impeded the Statistical Analysis tool. Because the *Methylobacterium vanA* genes
232 analyzed here originated from only the subset of metagenomes having >100 *vanA*
233 genes, the ratio of *Methylobacterium vanA* to all *vanA* was calculated using only the
234 metagenomes analyzed in that part of the study.
235
236
237 **Results**
238
239 **Genetic capacity for metabolism of methoxylated aromatic compounds is present**
240 **primarily in two clades of *Methylobacterium***
241 We searched the published genomes of 26 *Methylobacterium* strains for the presence
242 of *vanA*, *pcaG*, *pobA*, and *ech*. We found that all four genes are indeed present within
243 the genus *Methylobacterium*. They are primarily limited to two closely related clades,
244 the *aquaticum* clade and the *nodulans* clade; furthermore, they are present in nearly all
245 organisms in these clades (Fig. 1). However, there are exceptions. One member each
246 of the *extorquens* clade (*Methylobacterium sp.* AMS5) and the *radiotolerans* clade (*M.*
247 *pseudosasiacola*) also carry some aromatic catabolism genes (Fig. 1). Two members of
248 the *nodulans* clade (*sp.* 4-46 and *sp.* WSM2598) appear to lack *vanA,* though
249 *Methylobacterium sp*. 4-46 carries *ech* (Fig. 1) and *vdh* (not shown), conferring the
250 capacity to produce vanillate from ferulate, suggesting that the organism may have
251 previously had the capacity to utilize the product of these reactions but has since lost
252 *vanA*. Among the closest relatives to *Methylobacterium*, *Enterovirga rhinocerotis* has
253 none of the four genes of interest, and *Microvirga flocculans* has only *pobA* and *pcaH*.
254

255 Taken together, these patterns suggest that the capacity to metabolize several lignin-
256 derived aromatic compounds was acquired by the *aquaticum*/*nodulans* clade early in its
257 divergence within the *Methylobacterium*, but members of other clades have acquired
258 the genes more recently by horizontal gene transfer. To investigate this evolutionary
259 story further, we analyzed the phylogenies of the genes themselves, and also examined
260 the genomic contexts of *vanA* and *pcaG*.
261
262 **Phylogeny of aromatic catabolism genes supports ancestral origins in *M.***
263 ***aquaticum* and *M. nodulans* clades and horizontal acquisition by two other**
264 **species**
265 The phylogenies of *pobA*, *pcaG*, and *vanA* were largely congruent with the phylogeny of
266 conserved housekeeping genes within the *Methylobacterium* but not between
267 *Methylobacterium* and their closest relatives, supporting the hypothesis that the four
268 genes are ancestral to the *aquaticum*/*nodulans* clades but were not necessarily
269 acquired together (Fig. 2). The *ech* phylogeny was the most difficult to interpret, as the
270 *Methylobacterium* separated into three non-monophyletic clades (Fig. 2); it is possible
271 that not all gene homologs in the phylogeny code for enzymes specific to ferulate.
272 Notably, *Methylobacterium sp*. AMS5 and *M. pseudosasiacola* were more closely
273 related to each other than to any other species in both their *pobA* and *pcaG* sequences,
274 despite their phylogenetic distance from each other at the genome level. And while the
275 *pobA* sequences of those two strains fell within those of other *Methylobacterium*, their
276 *pcaG* sequences clustered with the *Sphingomonas*, further support not only for the
277 hypothesis that these two disparate species both acquired the beta-ketoadipate
278 pathway via horizontal gene transfer, but that they may have acquired it from the same
279 donor or that one served as the donor to the other.
280
281 **Gene synteny in *pcaG* and *vanA* neighborhoods is consistent with phylogeny**
282 We further examined the relationships of *vanA* and *pcaG* across species by comparing
283 patterns of synteny within the genome neighborhood for each. In all strains with *pcaG*,
284 the gene was located within a cluster of beta-ketoadipate pathway genes, and five of
285 these genes were present in all strains in the same order. Almost all strains also

286 contained a gene annotated as an uncharacterized conserved protein, DUF849
287 (COG3246, beta-keto acid cleavage enzyme), between *pcaG* and *pcaB* (Fig. 3). We
288 found no genes annotated as *pcaI* and *pcaJ* (beta-ketoadipate:succinyl-CoA
289 transferase) or *pcaF* (encoding beta-ketoadipyl-CoA thiolase) within these operons,
290 which are necessary for the final steps of the beta-ketoadipate pathway [5, 7]. All
291 *Methylobacterium* strains with *vanA* also had the other two genes required to confer the
292 ability for the demethoxylation of vanillate: *vanB* (encoding the other subunit of vanillate
293 monooxygenase) and *vanR* (an AraC family transcriptional regulator). Some strains also
294 had genes encoding a Major Facilitator Superfamily transporter specific to
295 protocatechuate (*pcaK*) or vanillate (*vanK*).
296
297 The genomic contexts of *pcaG* and *vanA* among strains exhibited patterns that agreed
298 overall with the phylogenies described above (Fig. 3). Closely related strains shared
299 common genes in the regions near *pcaG* and *vanA*, with differences among the strains
300 increasing with increasing distance from the genes of interest. Also consistent with
301 phylogeny, *Methylobacterium sp.* AMS5 and *M. pseudosasiacola* shared no
302 commonalities with the *M. aquaticum* clades or with each other in the neighborhoods
303 surrounding the *pca* genes or the *van* genes. Notably, in most previously described
304 organisms, the *pca* gene is not co-located with the other genes of interest in this study
305 (Tables S1, S2). However, the reaction product of the enzyme encoded by *pobA* (PCA)
306 is the substrate for the gene encoded by *pcaGH*; the proximity of the genes therefore
307 suggests that if these two organisms gained the *pca* genes via horizontal transfer, the
308 *pob* genes may have been transferred simultaneously as part of a catabolic island. We
309 found further support for the catabolic island hypothesis in the proximity of *vanA* and
310 *ech* to the *pca* genes in *Methylobacterium sp.* AMS5.
311
312 ***Methylobacterium sp*. AMS5 carries a catabolic island conferring the ability to**
313 **degrade lignin-derived aromatic compounds, in an *M. extorquens*-like genome**
314 The co-localization of all four aromatic catabolism genes of interest in the genome of
315 *Methylobacterium sp*. AMS5 prompted us to examine the region more closely. AMS5
316 was originally isolated in 2011 from the stem of a hypernodulating strain of soybean [51]

317 but is very closely related model organism *M. extorquens* PA1 [52, 53] (Fig. 1). We
318 aligned the two genomes, as well as that of another clade member, *M. zatmanii*
319 PSBB041, at the region where the aromatic catabolism genes are located (Fig. 4). The
320 comparison revealed that the region appears to be prone to the insertion and excision of
321 mobile genetic elements.
322
323 At the locus where *M. zatmanii* carries a gene encoding a putative IS5-type transposase
324 (possibly nonfunctional due to a frameshift with an internal stop codon), AMS5
325 contained an additional 22-kb region: a catabolic island containing genes that appear to
326 confer the full ability to degrade ferulate, vanillate, vanillin, *p*-hydroxybenzoate, and
327 protocatechuate, flanked by two different transposase genes from the MULE
328 superfamily. On the 3' side of this region, the two strains share 11 genes (14 kb), many
329 related to nucleotide sugar metabolism, that are also not present in PA1 (Fig. 4), or in
330 any of the other *Methylobacterium* species surveyed in this study. The corresponding
331 locus in the PA1 genome carries only a putative site-specific integrase/recombinase,
332 which is present only in the other *M. extorquens* strains (AM1, PA1, DM4; and *M.*
333 *chloromethanicum, M. populi,* which have previously been identified as *M. extorquens*
334 strains [54]). The gene adjacent to the integrase encodes UDP-*N*-acetylglucosamine 2-
335 epimerase (*wecB*); the sequence appears to be complete in *M. zatmanii* (1,137bp) but
336 truncated in PA1 (missing 912 bp from the 3' end). In all three genomes, the region of
337 variability lies immediately at the 3' end of the genes for tRNA-Pro and tRNA-Arg.
338
339 The presence of the truncated gene in PA1 suggests that the region of sugar
340 metabolism genes may originally have been present but were excised, whereas the
341 arrangement of genes in the catabolic island suggest it was acquired into a *M. zatmanii*-
342 like genomic background. The origins of the catabolic island itself are uncertain; as
343 shown above (Fig. 2), there appear to be diverse phylogenetic origins represented
344 among the different genes within the pathway, and BLAST search for the entire region
345 in the NCBI Nucleotide database found no other organisms containing all genes in the
346 same order. We could detect no genes in the region relating to replication or
347 conjugation as might be expected in an integrative and conjugative element (ICE) [55].

348 Furthermore, no significant difference in tetranucleotide composition or in GC content
349 was found between the inserted region (GC% = 71.4) and the full genome (GC% =
350 71.1) (Fig. S1), indicating that the catabolic island has likely been present in the
351 genome long enough for amelioration [56].
352
353 **Genome content predicts ability to grow on aromatic compounds in most**
354 ***Methylobacterium* strains**
355 We next wanted to assess whether *Methylobacterium* strains carrying genes for the
356 catabolism of methoxylated aromatic compounds could indeed use those compounds
357 as growth substrates. We chose 8 species from the *M. aquaticum*/*nodulans* clades,
358 shown in Figure 5 (and Table S1). All of these strains carry all four genes of interest
359 except *Methylobacterium sp.* 4-46, which lacks *vanA* and so was predicted not to grow
360 on vanillate or ferulate (Fig. 1). We conducted a series of growth experiments on
361 defined mineral medium with substrates of each of the four gene products of interest, as
362 well as succinate (a known growth substrate for all the strains tested), glucose (used by
363 only some *Methylobacterium* species), benzoic acid (another aromatic acid with a
364 degradation pathway separate from the beta-ketoadipate pathway [57]), vanillin, and
365 Kraft lignin (a soluble form of polymeric lignin). All strains grew on succinate and none
366 on lignin; growth on PHBA, PCA, vanillate, and ferulate was as expected for all strains
367 given their genome content, with the exceptions that *M. variabile* did not grow on
368 vanillate and *M. nodulans* did not grow on ferulate (Fig. 5, Fig. S2, Supplemental File
369 S2). No growth was observed on vanillin at the concentration tested; however, this may
370 be due in part to the toxicity of vanillin [58], as we have observed growth on vanillin by
371 *M. nodulans* when using lower concentrations in previous experiments.
372
373 **Non-methylotrophs excrete formaldehyde during vanillate growth, whereas**
374 ***Methylobacterium* do not**
375 We were especially interested to ask whether methylotrophs are different from non-
376 methylotrophs in their ability to cope with the formaldehyde produced during vanillate
377 metabolism. Although, as mentioned above, it is recognized that the formaldehyde
378 released by vanillate monooxygenase is a burden to organisms growing on vanillate, to

379 our knowledge no attempts have been made to measure the dynamics of accumulation
380 of the toxin during growth. We therefore measured formaldehyde in the medium during
381 the growth of two well-studied non-methylotrophic lignin degraders, *Pseudomonas*
382 *putida* KT2440 and *Rhodoccus jostii* RHA1: we assayed each strain on vanillate as well
383 as on PCA as a control compound, as PCA is the direct product of vanillate
384 demethylation and therefore involves the same metabolism except for the effect of
385 formaldehyde. In both strains, when growth occurred on vanillate, formaldehyde
386 accumulated in the medium concomitant with the increase in optical density, peaking at
387 concentrations of 0.94 mM (Fig. 6A, Table S4). When cultures entered stationary phase
388 (approximately 10 hours for *P. putida*, 15 hours for *R. jostii*), formaldehyde
389 concentrations began to decrease, ultimately returning to below the detection limit. No
390 formaldehyde was detected at any time during growth on PCA. Moreover, growth on
391 PCA was faster: stationary phase was reached at 7 hours for *P. putida* and 10 hours for
392 *R. jostii*. These results suggest that while both *P. putida* and *R. jostii* can oxidize
393 formaldehyde, removal is slower than production.
394
395 We conducted a similar experiment on the five strains of *Methylobacterium* showing the
396 greatest growth on vanillate in our laboratory conditions: *M. aquaticum*, *M. nodulans*, *M.*
397 *tarhaniae*, *Methylobacterium sp*. AMS5, and *M. aquaticum* MA-22A. We incubated all
398 cultures with vanillate for 33 hours, long enough for AMS5 to show marked growth and
399 all other species to consume all the substrate and reach stationary phase. No
400 detectable formaldehyde was produced at any time (Fig. 6B, Table S4). These results
401 suggest that *Methylobacterium* species are able to consume the formaldehyde
402 generated from vanillate demethylation as rapidly as it is produced, likely via the same
403 pathways by which the formaldehyde generated from methanol is used for energy
404 generation and biosynthesis.
405
406 ***Methylobacterium*-derived *vanA* reads in published metagenomes are**
407 **predominantly from the *M. nodulans* cluster, with highest relative abundance in**
408 **the phyllosphere**

409 Aside from the environments in which they were isolated (Table S1), there exists scant
410 information on the ecological niches of the aromatic-degrading *Methylobacterium*
411 clades—for instance, whether they are more likely than the other *Methylobacterium* to
412 inhabit ecosystems rich in lignin, such as soil or the rhizosphere. We therefore sought to
413 learn more about the prevalence and abundance of *vanA*-carrying *Methylobacterium*
414 species in the environment by querying the publicly available metagenome datasets on
415 the JGI IMG/M database. The distinctness of the *Methylobacterium* genes within the
416 phylogeny of known *vanA* sequences (Fig. 2) makes it possible to deduce phylogeny
417 from DNA sequence. *vanA* is present as a single copy in most genomes in which it is
418 found.
419
420 Our study set comprised 1,651 metagenomes, with a total assembled gene count of
421 5.60×10^9; we retrieved 317,816 scaffolds carrying *vanA*, of which 348 had
422 *Methylobacterium* as their IMG phylogenetic lineage assignment (a frequency of 0.11%)
423 (Tables S5, S6, S7). However, our phylogenetic placement using pplacer found that
424 only 182 of these genes actually fell within the *Methylobacterium* clades, whereas 31
425 clustered more closely with *Azospirillum halopraeferens*, and the remaining 135 were
426 distributed among more distantly related organisms (Fig. S4). We therefore focused
427 only on the genes identified by both IMG and pplacer as *Methylobacterium* for the
428 remainder of our analyses.
429
430 In absolute numbers, *vanA* genes belonging to *Methylobacterium* were highest in
431 samples from the soil (43% of *Methylobacterium vanA*) and rhizosphere/rhizoplane
432 (40%), the ecosystems in which *vanA* is most abundant generally (Fig. 7). However, we
433 were especially interested in environments where *Methylobacterium* are most prominent
434 within the community of vanillate degraders (high relative abundance of
435 *Methylobacterium vanA* genes among total *vanA*). We found that there were many
436 ecosystem types in which *vanA* was found but *Methylobacterium vanA* was not,
437 including engineered ecosystems and those associated with animal hosts (Table S5).
438 Where *Methylobacterium* were found, they made up the largest proportion of *vanA* in
439 phyllosphere/phylloplane samples (0.28±0.13% of *vanA* genes) (Fig. 7). Relative

440 abundances in the other ecosystem types were one order of magnitude lower
441 (freshwater: 0.024±0.016%; rhizoplane/rhizosphere: 0.022±0.010%; peat moss:
442 0.017%; soil: 0.014±0.005%; sediment: 0.011±0.005%, where ± denotes standard error;
443 only 1 peat moss genome contained *Methylobacterium vanA*). This distribution across
444 ecosystem types was qualitatively similar to that of total *Methylobacterium* reads in all
445 metagenomes (Fig. 7).
446
447 The metagenome sequences identified as *Methylobacterium vanA* fell into three
448 phylogenetic clusters (Fig. 8). The majority (114 genes, 63%) were most closely related
449 to *M. nodulans*; 17% (31 genes) clustered with *Methylobacterium sp*. AMS5, and 20%
450 (37 genes) clustered with the remaining *vanA*-carrying species, in the *M. aquaticum*
451 clade (Fig. 8). These three clades were distributed approximately evenly across all
452 ecosystem types.
453
454
455 **Discussion**
456
457 We have provided the first comprehensive description of growth of *Methylobacterium* on
458 lignin-derived methoxylated aromatic acids. *Methylobacterium* species with this
459 capability can use vanillate as a sole carbon substrate without the transient
460 formaldehyde accumulation in the environment that is observed with non-methylotrophic
461 vanillate degraders. The genes encoding aromatic catabolism are found almost
462 exclusively in all members of the *M. aquaticum* and *M. nodulans* clades, but acquisition
463 by horizontal gene transfer has been observed in other *Methylobacterium* species.
464 These findings shed new light on the ecology of the genus.
465
466 Although there are important implications for our understanding of the bacterial lignin-
467 degrading community, we are far from proposing that *Methylobacterium* be classified as
468 lignin degraders: the species we studied were not found to grow on Kraft lignin, nor is
469 there evidence that *Methylobacterium* can produce the peroxidases or laccases
470 necessary for lignin depolymerization. In the environment, these organisms may depend

471 upon aromatic acids released by the action of other lignin-degrading organisms, which
472 have been found to be a prominent component of leaf litter leachate [59]. Alternatively,
473 *Methylobacterium* may encounter these compounds primarily in plant root exudates
474 [60]. In addition to acting as a growth substrate, aromatic acids play an important role in
475 plant-microbe signaling: vanillate, ferulate, *p*-hydroxybenzoate, and protocatechuate all
476 influence on the process and productivity of root nodulation by other members of the
477 *Rhizobiales* [61, 62]. This is significant in light of the fact that the members of the *M.*
478 *nodulans* clade were, as the species name suggests, isolated from root and stem
479 nodules of their plant hosts [21, 63]; and that we found this clade to be the most
480 abundant among the *Methylobacterium vanA* genes found in the environment.
481 Furthermore, *Methylobacterium sp*. AMS5 was isolated in a study on soybean epiphytes
482 that are particularly responsive to host nodulation phenotype [51]. It is likely that at least
483 part of the importance of aromatic catabolism in the *Methylobacterium* is to facilitate the
484 relationships of these plant-associated organisms with their hosts. A link between
485 aromatic catabolism and plant-microbe symbioses could help to explain our finding that
486 organisms from the *M. nodulans* and *Methylobacterium sp*. AMS5 clades are dominant
487 among the *Methylobacterium vanA* sequences found in the environment, despite the
488 fact that there are few genome-sequenced representatives.
489
490 Perhaps the most compelling results from this study are the new insights into the
491 evolution of the genus *Methylobacterium*. One element is the absence of the *vanA* gene
492 in *Methylobacterium sp*. 4-46 and *sp.* WSM298, the only two species in the *M.*
493 *nodulans*/ *M. aquaticum* clades to lack the capacity for methoxydotrophic growth. These
494 species do carry genes for transforming ferulate to vanillin (*ech*) and vanillin to vanillate
495 (*vdh*), which may be remnants from predecessors that were able to metabolize vanillate
496 but lost the capability. Notably, *Methylobacterium* sp. 4-46 is also one of very few
497 *Methylobacterium* species reported to be unable to grow on methanol [64]; our lab has
498 found that it can indeed use methanol as a growth substrate but only in the presence of
499 $LaCl_3$ (Fig. S5, Table S8), suggesting the involvement of a XoxF-type methanol
500 dehydrogenase [44], and possibly a different role for methanol oxidation in this
501 organism's ecology. Given our hypothesis that methanol oxidation and vanillate

502 demethylation require the same pathways for metabolizing the formaldehyde produced,
503 it is possible that the loss of *vanA* in *Methylobacterium* sp. 4-46 might be related to its
504 different style of methylotrophy. We have also observed that this and several non-
505 *Methylobacterium* lignin-degrading species possess the genes to use PCA (the
506 aromatic product of vanillate demethylation) but not the methoxy group (Fig. 1). Yet we
507 have found no species in which the reverse is true, although it would theoretically be
508 possible for a methylotroph with *van* genes but no *pca* genes to carry out
509 methoxydotrophic growth by utilizing only the methoxy group of vanillate.
510
511 The other unexpected evolutionary finding relates to the acquisition of aromatic
512 catabolism genes by horizontal transfer in two *Methylobacterium* species from outside
513 of the *M. nodulans*/*aquaticum* clades. The discovery of a catabolic island in
514 *Methylobacterium sp.* AMS5 is itself not unusual; *Methylobacterium* species have long
515 been recognized to carry an abundance of IS (insertion sequence) elements, and it has
516 been postulated that the associated genome rearrangements and horizontal gene
517 transfer associated are important mechanisms of evolution in the genus [65–67].
518 Relevant to the present study is the prior observation that diverse features of the
519 genomic background—and not necessarily those predicted by phylogeny—influence
520 whether a newly introduced set of genes are immediately useful to the recipient
521 organism [68]. Are there particular features of the *M. pseudosasiacola* and
522 *Methylobacterium sp.* AMS5 genomes that allowed them to acquire the capacity for the
523 degradation of methoxylated aromatics when no other known members of their clades
524 did, or is the maintenance of this genomic capability the result of selective pressure
525 specific to their ecological niche? Further work on the ecology of AMS5 and the biology
526 of aromatic catabolism in *Methylobacterium* is necessary to address these questions.
527
528 This study has benefited from the wealth of knowledge that already exists on microbial
529 degradation pathways for the degradation of lignin-derived aromatics in other
530 organisms, and on methylotrophic metabolism in *Methylobacterium*, to deduce the likely
531 fate of the methoxy group from vanillate. We found that in most cases, the gene
532 annotations in IMG enabled us to correctly predict the substrates each strain could grow

533 on (the two exceptions were both cases of no growth, and we cannot rule out the
534 possibility that growth could occur under different conditions). However, we did find
535 some novel features of the *Methylobacterium* pathways: almost all the strains we
536 studied appear have no homologs of *pcaI*, *pcaJ, or pcaF* encoded within the *pca* gene
537 cluster. It is possible that the functions of these genes are carried out by homologs
538 located elsewhere in the genome, as has been found in some other organisms [6]. A
539 second possibility is raised by a previous study that carried out enzymatic screening
540 and active site modeling on the DUF849 family of genes [69]: several of the DUF849
541 genes found in these *Methylobacterium* gene clusters were classified as beta-keto acid
542 cleavage enzymes (G4 BKACE) predicted to act on betaketoadipate, raising the
543 possibility that they might carry out the *pcaI/pcaJ* function and thus constitute a novel
544 variant of the already diverse family of beta-ketoadipate pathway configurations [6, 7].
545
546 Likewise, our work benefited from the abundance of metagenome data that are publicly
547 available, as a way of achieving a broad overview of the ecology our organisms of
548 interest. However, *Methylobacterium* likely make up ~0.01-0.2% of organisms carrying
549 *vanA* in environments where vanillate degraders are found; this low abundance means
550 that even searching the entire set of available data on IMG/M yielded only 182 gene
551 sequences of interest, and the majority of metagenomes with *Methylobacterium vanA*
552 genes contained only one such gene, making statistical analysis difficult. Furthermore,
553 the very environment where *Methylobacterium* make up a greater part of the *vanA*
554 population is that where total *vanA* reads are low and therefore poorly represented in
555 our dataset: the phyllosphere. Taken together, these caveats mean that the broad-scale
556 ecological patterns observed in this initial survey should be interpreted with caution.
557 However, as the first such survey carried out, our work provides a dataset on which to
558 base more targeted assays to obtain a deeper understanding of the diversity and
559 distribution of aromatic-degrading *Methylobacterium* in the environment.
560

Acknowledgments

We are grateful to Nicholas Shevalier, Alyssa Baugh, and Tomislav Ticak for their assistance with experiments and support during the scientific process. We thank Armando MacDonald for technical assistance with measurements, Akio Tani for providing the *M. aquaticum* MA-22A culture, Andrea Lubbe and Trent Northen for the *P. putida* and *R. jostii* cultures, and José de la Torre for assistance with calculating genome signatures. We are thankful to Dipti Nayak, Mete Yuksel, Elizabeth Winters, Brittany Baker, and Tomislav Ticak for their valuable feedback on the manuscript. This work was funded by grants from the US Department of Energy Genomic Science Program in Systems Biology for Energy and Environment, award DE-SC0012627, and from the US National Science Foundation Dimensions of Biodiversity Program, award DEB-1831838.

575 **References**

576

577 1. Ragauskas AJ, Beckham GT, Biddy MJ, Chandra R, Chen F, Davis MF, et al.
578 Lignin valorization: Improving lignin processing in the biorefinery. *Science* 2014;
579 **344**: 1246843.
580 2. Welte CU. A microbial route from coal to gas. *Science* 2016; **354**: 184–184.
581 3. Ruiz-Dueñas FJ, Martínez ÁT. Microbial degradation of lignin: how a bulky
582 recalcitrant polymer is efficiently recycled in nature and how we can take
583 advantage of this. *Microb Biotechnol* 2009; **2**: 164–177.
584 4. Vanholme R, Demedts B, Morreel K, Ralph J, Boerjan W. Lignin biosynthesis and
585 structure. *Plant Physiology* 2010; **153**: 895–905.
586 5. Harwood CS, Parales RE. The beta-ketoadipate pathway and the biology of self-
587 identity. *Annu Rev Microbiol* 1996; **50**: 553–590.
588 6. Parke D. Acquisition, reorganization, and merger of genes: novel management of
589 the β-ketoadipate pathway in *Agrobacterium tumefaciens*. *FEMS Microbiol Lett*
590 1997; **146**: 3–12.
591 7. Buchan A, Neidle EL, Moran MA. Diverse organization of genes of the β-
592 ketoadipate pathway in members of the marine *Roseobacter* lineage. *Appl Environ*
593 *Microbiol* 2004; **70**: 1658–1668.
594 8. Brunel F, Davison J. Cloning and sequencing of *Pseudomonas* genes encoding
595 vanillate demethylase. *J Bacteriol* 1988; **170**: 4924–4930.
596 9. Mitsui R, Kusano Y, Yurimoto H, Sakai Y, Kato N, Tanaka M. Formaldehyde
597 fixation contributes to detoxification for growth of a nonmethylotroph, *Burkholderia*
598 *cepacia* TM1, on vanillic acid. *Appl Environ Microbiol* 2003; **69**: 6128–6132.

599 10. Merkens H, Beckers G, Wirtz A, Burkovski A. Vanillate metabolism in
600 *Corynebacterium glutamicum*. *Curr Microbiol* 2005; **51**: 59–65.
601 11. Sudtachat N, Ito N, Itakura M, Masuda S, Eda S, Mitsui H, et al. Aerobic vanillate
602 degradation and C1 compound metabolism in *Bradyrhizobium japonicum*. *Appl*
603 *Environ Microbiol* 2009; **75**: 5012–5017.
604 12. Chen H-P, Chow M, Liu C-C, Lau A, Liu J, Eltis LD. Vanillin catabolism in
605 *Rhodococcus jostii* RHA1. *Appl Environ Microbiol* 2012; **78**: 586–588.
606 13. Chen NH, Djoko KY, Veyrier FJ, McEwan AG. Formaldehyde stress responses in
607 bacterial pathogens. *Front Microbiol* 2016; **7**.
608 14. Hibi M, Sonoki T, Mori H. Functional coupling between vanillate-O-demethylase
609 and formaldehyde detoxification pathway. *FEMS Microbiol Lett* 2005; **253**: 237–
610 242.
611 15. Lessmeier L, Hoefener M, Wendisch VF. Formaldehyde degradation in
612 *Corynebacterium glutamicum* involves acetaldehyde dehydrogenase and
613 mycothiol-dependent formaldehyde dehydrogenase. *Microbiology* 2013; **159**:
614 2651–2662.
615 16. Roca A, Rodríguez-Herva JJ, Ramos JL. Redundancy of enzymes for
616 formaldehyde detoxification in *Pseudomonas putida*. *J Bacteriol* 2009; **191**: 3367–
617 3374.
618 17. Kato N, Yurimoto H, Thauer RK. The physiological role of the ribulose
619 monophosphate pathway in bacteria and archaea. *Biosci Biotechnol Biochem*
620 2006; **70**: 10–21.

621 18. Mayumi D, Mochimaru H, Tamaki H, Yamamoto K, Yoshioka H, Suzuki Y, et al.
622 Methane production from coal by a single methanogen. *Science* 2016; **354**: 222–
623 225.
624 19. Chistoserdova L. Modularity of methylotrophy, revisited. *Environmental*
625 *Microbiology* 2011; **13**: 2603–2622.
626 20. Ito H, Iizuka H. Taxonomic studies on a radio-resistant *Pseudomonas*. *Agric Biol*
627 *Chem* 1971; **35**: 1566–1571.
628 21. Jourand P. *Methylobacterium nodulans* sp. nov., for a group of aerobic,
629 facultatively methylotrophic, legume root-nodule-forming and nitrogen-fixing
630 bacteria. *Int J Syst Evol Biol* 2004; **54**: 2269–2273.
631 22. Ventorino V, Sannino F, Piccolo A, Cafaro V, Carotenuto R, Pepe O.
632 *Methylobacterium populi* VP2: plant growth-promoting bacterium isolated from a
633 highly polluted environment for polycyclic aromatic hydrocarbon (PAH)
634 biodegradation. *Sci World J* 2014; **2014**.
635 23. Masai E, Katayama Y, Fukuda M. Genetic and biochemical investigations on
636 bacterial catabolic pathways for lignin-derived aromatic compounds. *Biosci*
637 *Biotechnol Biochem* 2007; **71**: 1–15.
638 24. Kelly DP, McDonald IR, Wood AP. The family *Methylobacteriaceae*. In: Rosenberg
639 E, DeLong EF, Lory S, Stackebrandt E, Thompson F (eds). *The Prokaryotes*, 4th
640 ed. 2014. Springer Berlin Heidelberg, pp 313–340.
641 25. Chen I-MA, Chu K, Palaniappan K, Pillay M, Ratner A, Huang J, et al. IMG/M v.5.0:
642 an integrated data management and comparative analysis system for microbial
643 genomes and microbiomes. *Nucleic Acids Res* 2019; **47**: D666–D677.

644 26. Green PN, Ardley JK. Review of the genus *Methylobacterium* and closely related
645 organisms: a proposal that some *Methylobacterium* species be reclassified into a
646 new genus, *Methylorubrum* gen. nov. *Int J Syst Evol Microbiol* 2018; **68**: 2727–
647 2748.
648 27. Parte AC. LPSN – List of prokaryotic names with standing in nomenclature
649 (bacterio.net), 20 years on. *Int J Syst Evol Microbiol* 2018; **68**: 1825–1829.
650 28. Menna P, Barcellos FG, Hungria M. Phylogeny and taxonomy of a diverse
651 collection of *Bradyrhizobium* strains based on multilocus sequence analysis of the
652 16S rRNA gene, ITS region and *glnII, recA, atpD* and *dnaK* genes. *International*
653 *Journal of Systematic and Evolutionary Microbiology* 2009; **59**: 2934–2950.
654 29. Zhang YM, Tian CF, Sui XH, Chen WF, Chen WX. Robust markers reflecting
655 phylogeny and taxonomy of rhizobia. *PLOS ONE* 2012; **7**: e44936.
656 30. Gaunt MW, Turner SL, Rigottier-Gois L, Lloyd-Macgilp SA, Young JP. Phylogenies
657 of *atpD* and *recA* support the small subunit rRNA-based classification of rhizobia.
658 *International Journal of Systematic and Evolutionary Microbiology* 2001; **51**: 2037–
659 2048.
660 31. Sievers F, Wilm A, Dineen D, Gibson TJ, Karplus K, Li W, et al. Fast, scalable
661 generation of high-quality protein multiple sequence alignments using Clustal
662 Omega. *Mol Syst Biol* 2011; **7**: 539.
663 32. Nguyen L-T, Schmidt HA, von Haeseler A, Minh BQ. IQ-TREE: A fast and effective
664 stochastic algorithm for estimating maximum-likelihood phylogenies. *Mol Biol Evol*
665 2015; **32**: 268–274.

666 33. Miller MA, Pfeiffer W, Schwartz T. Creating the CIPRES Science Gateway for
667 inference of large phylogenetic trees. *Proceedings of the Gateway Computing*
668 *Environments Workshop (GCE)*. 2010. New Orleans, LA, pp 1–8.
669 34. Anisimova M, Gascuel O. Approximate likelihood-ratio test for branches: A fast,
670 accurate, and powerful alternative. *Syst Biol* 2006; **55**: 539–552.
671 35. Darling ACE, Mau B, Blattner FR, Perna NT. Mauve: Multiple alignment of
672 conserved genomic sequence with rearrangements. *Genome Res* 2004; **14**: 1394–
673 1403.
674 36. Darling AE, Mau B, Perna NT. progressiveMauve: Multiple genome alignment with
675 gene gain, loss and rearrangement. *PLOS ONE* 2010; **5**: e11147.
676 37. Guy L, Roat Kultima J, Andersson SGE. genoPlotR: comparative gene and
677 genome visualization in R. *Bioinformatics* 2010; **26**: 2334–2335.
678 38. R Core Team. R: A language and environment for statistical computing. 2018. R
679 Foundation for Statistical Computing, Vienna, Austria.
680 39. RStudio. 2018. RStudio, Boston, MA.
681 40. Pagès H, Aboyoun P, Gentleman R, DebbRoy S. Biostrings: Efficient manipulation
682 of biological strings. 2019.
683 41. Karlin S. Detecting anomalous gene clusters and pathogenicity islands in diverse
684 bacterial genomes. *Trends Microbiol* 2001; **9**: 335–343.
685 42. Delaney NF, Kaczmarek ME, Ward LM, Swanson PK, Lee M-C, Marx CJ.
686 Development of an optimized medium, strain and high-throughput culturing
687 methods for *Methylobacterium extorquens*. *PLOS ONE* 2013; **8**: e62957.

688 43. Atlas RM. Handbook of Microbiological Media, Fourth Edition, 4 edition. 2010. CRC
689 Press, Washington, D.C. : Boca Raton, FL.
690 44. Skovran E, Martinez-Gomez NC. Just add lanthanides. *Science* 2015; **348**: 862–
691 863.
692 45. Nash T. The colorimetric estimation of formaldehyde by means of the Hantzsch
693 reaction. *Biochem J* 1953; **55**: 416–421.
694 46. Huntemann M, Ivanova NN, Mavromatis K, Tripp HJ, Paez-Espino D, Tennessen
695 K, et al. The standard operating procedure of the DOE-JGI Metagenome
696 Annotation Pipeline (MAP v.4). *Standards in Genomic Sciences* 2016; **11**: 17.
697 47. Matsen FA, Kodner RB, Armbrust EV. pplacer: linear time maximum-likelihood and
698 Bayesian phylogenetic placement of sequences onto a fixed reference tree. *BMC*
699 *Bioinformatics* 2010; **11**: 538.
700 48. Eddy SR. HMMER - biosequence analysis using profile hidden Markov models.
701 2007.
702 49. Stamatakis A. RAxML version 8: a tool for phylogenetic analysis and post-analysis
703 of large phylogenies. *Bioinformatics* 2014; **30**: 1312–1313.
704 50. McMurdie PJ, Holmes S. phyloseq: an R package for reproducible interactive
705 analysis and graphics of microbiome census data. *PLOS ONE* 2013; **8**: e61217.
706 51. Anda M, Ikeda S, Eda S, Okubo T, Sato S, Tabata S, et al. Isolation and genetic
707 characterization of *Aurantimonas* and *Methylobacterium* strains from stems of
708 hypernodulated soybeans. *Microbes Environ* 2011; **26**: 172–180.

709 52. Nayak DD, Marx CJ. Genetic and phenotypic comparison of facultative
710 methylotrophy between *Methylobacterium extorquens* strains PA1 and AM1. *PLoS*
711 *ONE* 2014; **9**: e107887.
712 53. Knief C, Frances L, Vorholt JA. Competitiveness of diverse *Methylobacterium*
713 strains in the phyllosphere of *Arabidopsis thaliana* and identification of
714 representative models, including *M. extorquens* PA1. *Microb Ecol* 2010; **60**: 440–
715 452.
716 54. Marx CJ, Bringel F, Chistoserdova L, Moulin L, Farhan Ul Haque M, Fleischman
717 DE, et al. Complete genome sequences of six strains of the genus
718 *Methylobacterium*. *J Bacteriol* 2012; **194**: 4746–4748.
719 55. Wozniak RAF, Waldor MK. Integrative and conjugative elements: mosaic mobile
720 genetic elements enabling dynamic lateral gene flow. *Nat Rev Microbiol* 2010; **8**:
721 552–563.
722 56. Lawrence JG, Ochman H. Amelioration of bacterial genomes: Rates of change and
723 exchange. *J Mol Evol* 1997; **44**: 383–397.
724 57. Moreno R, Rojo F. The target for the *Pseudomonas putida* Crc global regulator in
725 the benzoate degradation pathway is the *BenR* transcriptional regulator. *J Bacteriol*
726 2008; **190**: 1539–1545.
727 58. Fitzgerald DJ, Stratford M, Gasson MJ, Ueckert J, Bos A, Narbad A. Mode of
728 antimicrobial action of vanillin against *Escherichia coli*, *Lactobacillus plantarum* and
729 *Listeria innocua*. *J Appl Microbiol* 2004; **97**: 104–113.
730 59. Kuiters AT. Role of phenolic substances from decomposing forest litter in plant–soil
731 interactions. *Acta Botanica Neerlandica* 1990; **39**: 329–348.

732 60. Zhalnina K, Louie KB, Hao Z, Mansoori N, Rocha UN da, Shi S, et al. Dynamic root
733 exudate chemistry and microbial substrate preferences drive patterns in
734 rhizosphere microbial community assembly. *Nat Microbiol* 2018; **3**: 470–480.
735 61. Mandal SM, Chakraborty D, Dey S. Phenolic acids act as signaling molecules in
736 plant-microbe symbioses. *Plant Signal Behav* 2010; **5**: 359–368.
737 62. Seneviratne G, Jayasinghearachchi HS. Phenolic acids: Possible agents of
738 modifying N_2-fixing symbiosis through rhizobial alteration? *Plant and Soil* 2003;
739 **252**: 385–395.
740 63. Fleischman D, Kramer D. Photosynthetic rhizobia. *Biochim Biophys Acta Bioeng*
741 1998; **1364**: 17–36.
742 64. Ardley JK, O'Hara GW, Reeve WG, Yates RJ, Dilworth MJ, Tiwari RP, et al. Root
743 nodule bacteria isolated from South African *Lotononis bainesii*, *L. listii* and *L.*
744 *solitudinis* are species of *Methylobacterium* that are unable to utilize methanol.
745 *Arch Microbiol* 2009; **191**: 311–318.
746 65. Vuilleumier S, Chistoserdova L, Lee M-C, Bringel F, Lajus A, Zhou Y, et al.
747 *Methylobacterium* genome sequences: A reference blueprint to investigate
748 microbial metabolism of C1 compounds from natural and industrial sources. *PLOS*
749 *ONE* 2009; **4**: e5584.
750 66. Schmid-Appert M, Zoller K, Traber H, Vuilleumier S, Leisinger T. Association of
751 newly discovered IS elements with the dichloromethane utilization genes of
752 methylotrophic bacteria. *Microbiology* 1997; **143**: 2557–2567.
753 67. Nayak DD, Marx CJ. Experimental horizontal gene transfer of methylamine
754 dehydrogenase mimics prevalent exchange in nature and overcomes the

755 methylamine growth constraints posed by the sub-optimal N-methylglutamate
756 pathway. *Microorganisms* 2015; **3**: 60–79.
757 68. Michener JK, Vuilleumier S, Bringel F, Marx CJ. Phylogeny poorly predicts the
758 utility of a challenging horizontally transferred gene in *Methylobacterium* strains. *J*
759 *Bacteriol* 2014; **196**: 2101–2107.
760 69. Bastard K, Smith AAT, Vergne-Vaxelaire C, Perret A, Zaparucha A, De Melo-
761 Minardi R, et al. Revealing the hidden functional diversity of an enzyme family.
762 *Nature Chemical Biology* 2014; **10**: 42–49.
763

764 **Figures and legends**

765

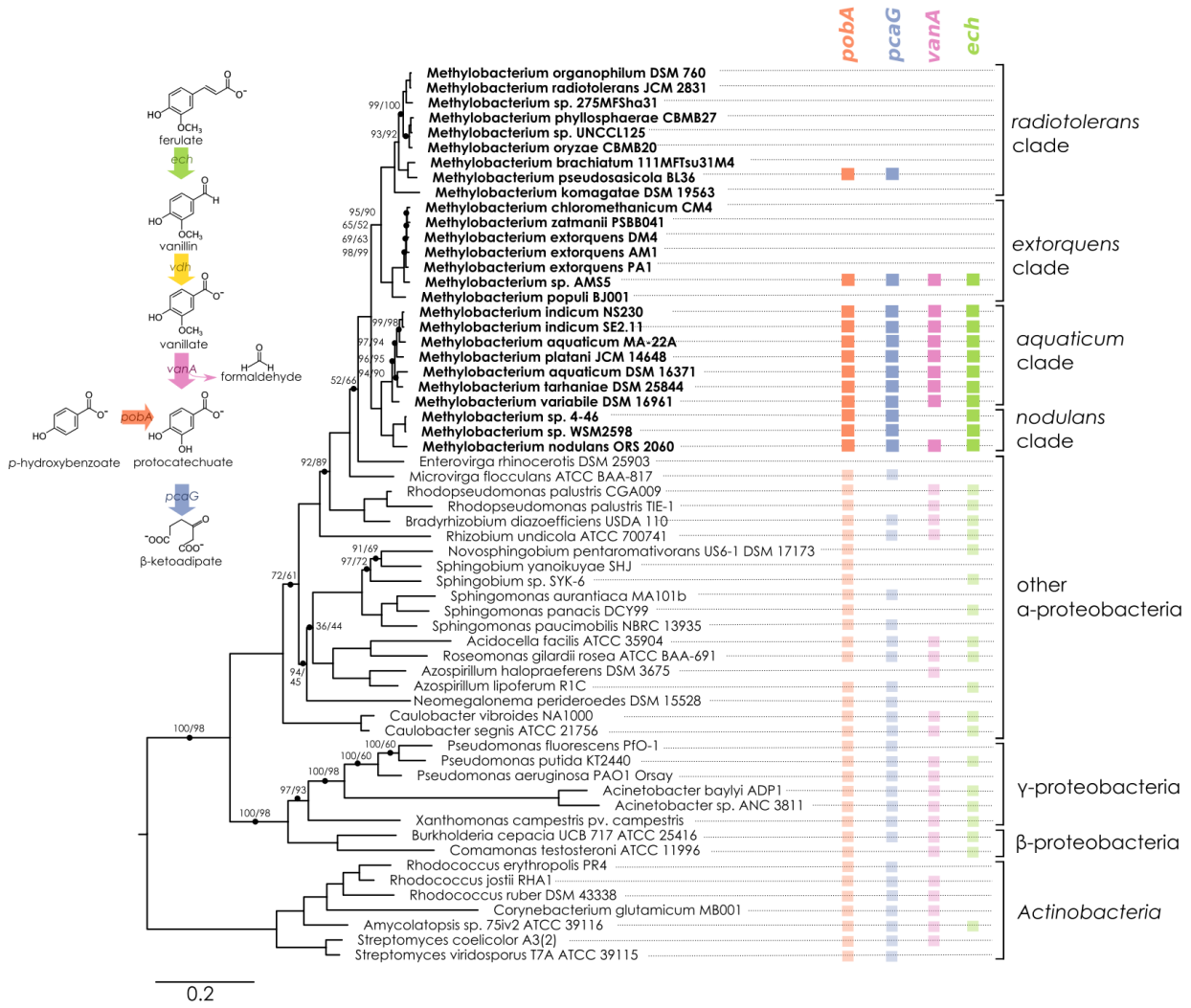

766

767

768 **Figure 1. Genes associated with aromatic catabolism are present in two clusters of**
769 **closely-related *Methylobacterium* species, with some exceptions.**
770 Genomes of *Methylobacterium* species and known aromatic-degrading bacteria were
771 searched for four genes involved in different steps of the degradation of lignin-derived
772 methoxylated aromatic compounds (upper left). Colored squares indicate the presence
773 of each gene. Among the reference organisms (not *Methylobacterium*), all species that
774 do not have *pcaG* do have the genes for protocatechuate 4,5-dioxygenase, indicating an
775 alternative ring cleavage mechanism and different pathway for the catabolism of PCA.
776 The phylogeny was composed using a concatenated alignment of four housekeeping
777 genes (*atpD, recA, rpob*, and 16S rRNA), with the cyanobacterium species
778 Prochlorococcus marinus as an outgroup (not shown). Branch labels indicate SH-aLRT
779 branch support/ UltraFast bootstrap values; all unlabeled branches have values of
780 100/100. Accession numbers and published references are given in Tables S1 and S2.

781

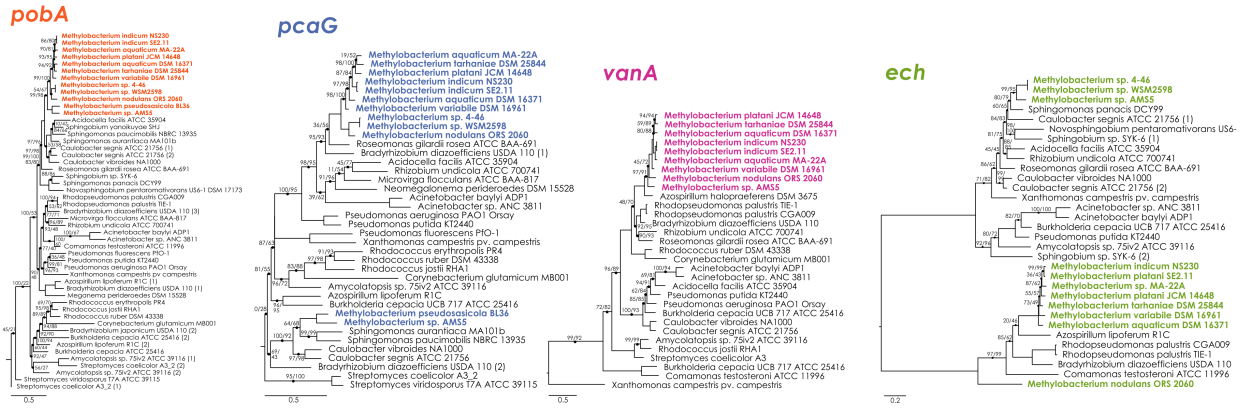

Figure 2. Phylogenies of aromatic catabolism genes suggest all four are ancestral to the *M. aquaticum/nodulans* clades, and have been horizontally acquired by two other *Methylobacterium* species.

For all organisms in Fig. 1, the sequences of *pobA* (*p*-hydroxybenzoate 3-monooxygenase), *pcaH* (protocatechuate 3,4-dioxygenase beta subunit), *vanA (*vanillate monooxygenase subunit A), and *ech* (*trans*-feruloyl-CoA hydratase/vanillin synthase) were aligned and phylogenies constructed using maximum likelihood, with homologs from archaeal organisms as outgroups (not shown). Accession numbers for all genes are given in Tables S1 and S2. Branch labels indicate SH-aLRT branch support/UltraFast bootstrap values; all unlabeled branches have values of 100/100. Comparison of these phylogenies and that in Fig. 1 suggest that all four genes are restricted to and prevalent in the *M. aquaticum* and *M. nodulans* clades, with a few losses (*vanA* by *Methylobacterium sp*. 4-46 and WSM2598) and some gains by horizontal gene transfer (in *M. pseudosasiacola* and *Methylobacterium sp*. AMS-5).

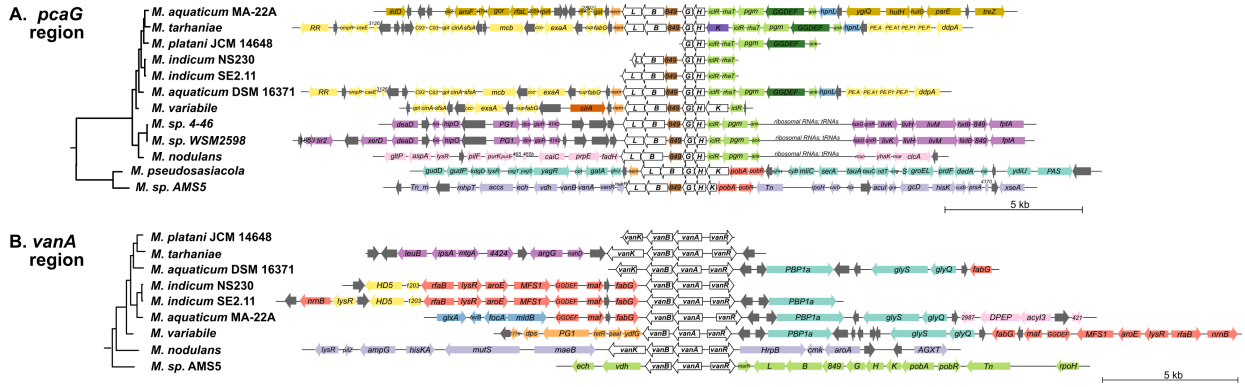

Figure 3. Genomic context of *vanA* and *pcaG* genes in *Methylobacterium* species supports a common evolutionary origin within the *M. aquaticum/nodulans* clades and separate origin in *M. pseudosasiacola* and *Methylobacterium sp.* AMS-5. Genomic regions (from fully assembled genomes) or scaffolds (from partially assembled genomes) are shown with A) all *pcaG* genes aligned or B) all *vanA* genes aligned. Gene phylogenies are excerpted from Fig. 2. Genes related to the beta-ketoadipate pathway (in A) and to vanillate demethylation (in B) are shown in white. Homologous regions shared across multiple genomes are shown in the same color to facilitate comparison among genomes. Gene labels are abbreviations based on functional annotations; full information on all genes is given in Table S3. Members of the *M. aquaticum* and *M. nodulans* clades share some synteny in the regions surrounding the *van* and *pca* gene clusters, with the degree of synteny roughly paralleling their phylogenetic distance; as an exception, *Methylobacterium sp.* AMS-5 and *M. pseudosasiacola* differ markedly from the other species.

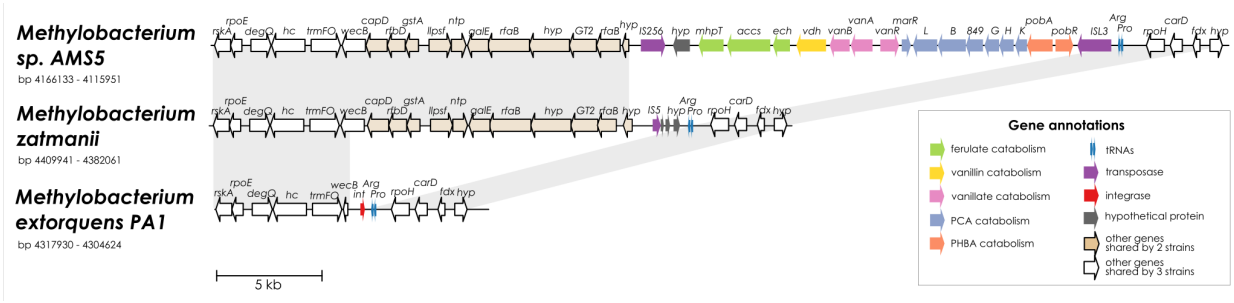

Figure 4. Alignment of three genomes from the *M. extorquens* clade reveals that *Methylobacterium sp*. AMS-5 harbors a catabolic island conferring the ability to degrade several aromatic substrates, in a genomic region prone to insertions and deletions.

The genome of *Methylobacterium sp*. AMS5 is shown aligned with that of two close relatives, *M. zatmanii* PSBB041 and *M. extorquens* PA1. Genes are color-coded to indicate function or commonality between genomes, as indicated by the key. Light gray shading between pairs of species connects regions shared by both. See Table S3 for full annotations corresponding to the short gene codes.

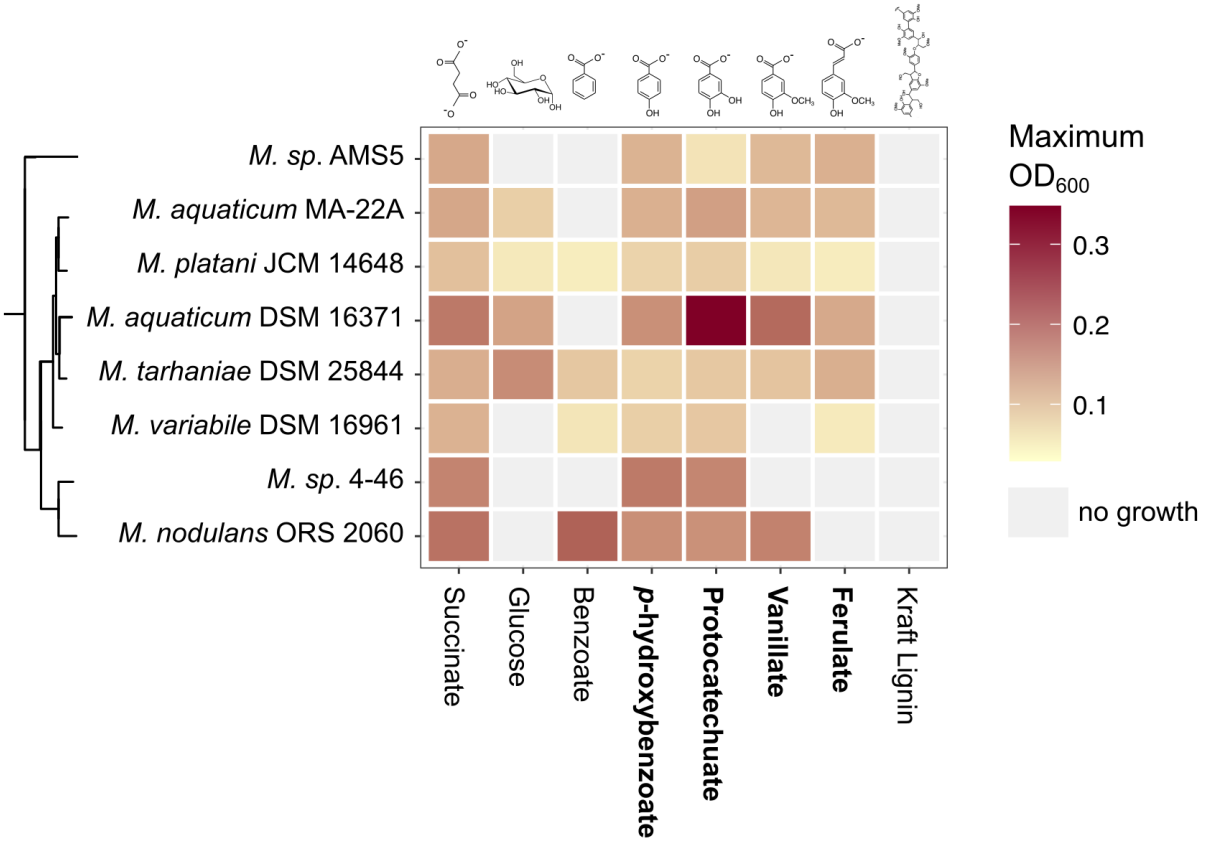

Figure 5. Growth of *Methylobacterium* species on aromatic compounds is predicted by genetic potential in most cases.
Methylobacterium species were grown in defined mineral medium with a single carbon substrate; all conditions contained 16 mM of carbon. Substrates corresponding to the four degradation pathways featured in this study are in bold; all species tested have genetic capacity for all four aromatic substrates except in the case of *Methylobacterium sp*. 4-46 and vanillate. Shading indicates maximum optical density (OD) at 600 nm measured during 80 hours of incubation, the average of three biological replicates. Original growth curves are shown in Fig. S2.

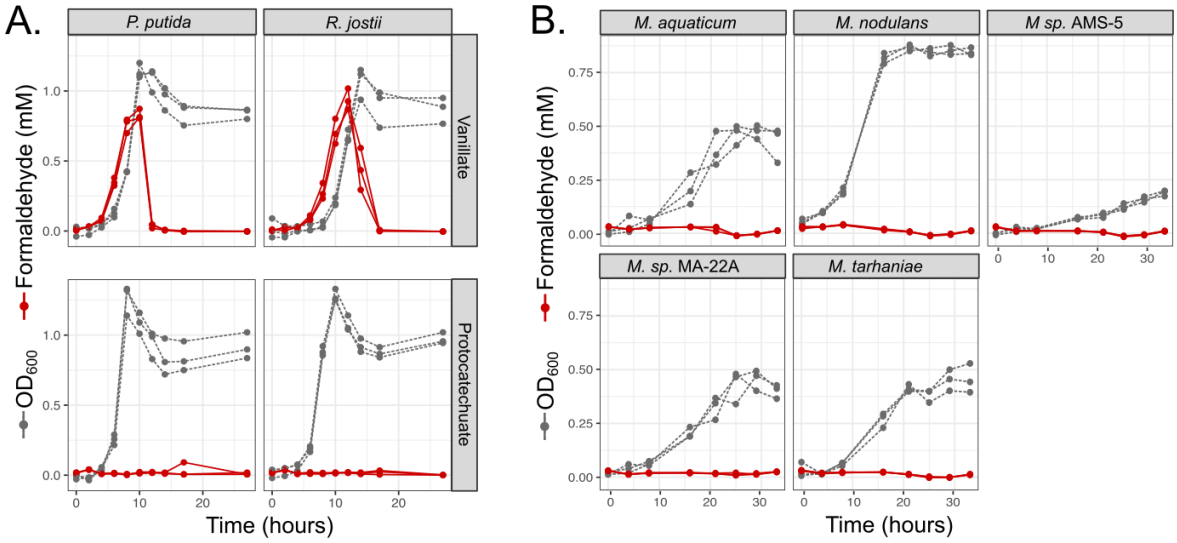

Figure 6. Non-methylotrophic lignin degraders *Pseudomonas putida* and *Rhodococcus jostii* produce formaldehyde when growing on methoxy-substituted aromatic compounds such as vanillate; *Methylobacterium* do not.
All organisms were grown in defined mineral medium with vanillate or protocatechuate (PCA) as a sole carbon source; growth was assayed by optical density at 600 nm (gray symbols and dashed lines) and formaldehyde in the medium was measured by a colorimetric assay (red symbols and solid lines). Each line represents one biological replicate. A) *P. putida* and *R. jostii* accumulate formaldehyde transiently in the medium when growing on vanillate, but not on the non-methoxylated compound PCA, and growth is slower on vanillate. B) All *Methylobacterium* species tested grew on vanillate without producing measurable formaldehyde.

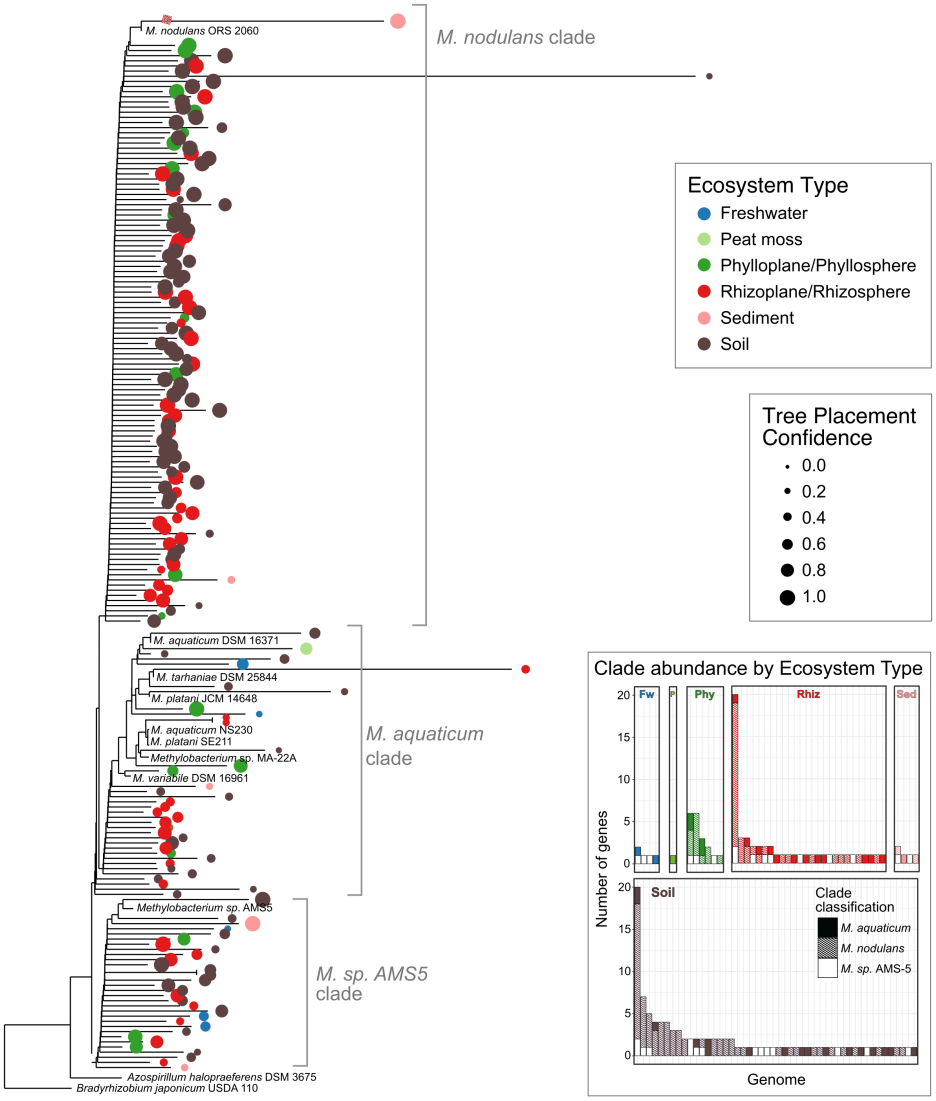

Figure 7. Organisms carrying *vanA* are most abundant in peat moss, rhizosphere, and soil; *Methylobacterium* are most abundant in the phyllosphere both overall and among *vanA*-carrying organisms.
Relative abundances of A) *vanA* genes and B*) Methylobacterium* genes as a percentage of all genes in each metagenome in the IMG/M database at the time of study. The numbers above each bar give the number of metagenomes searched in each ecosystem type (all metagenomes contained both *vanA* genes and *Methylobacterium* genes). C) Relative abundance of *Methylobacterium vanA* genes as a percentage of all *vanA* genes. The fraction above each bar denotes the number of metagenomes in which *Methylobacterium vanA* genes were found over the number of metagenomes searched for that ecosystem type (metagenomes were only searched if they had >100 *vanA* genes). Error bars denote the standard error among all metagenomes in the set.

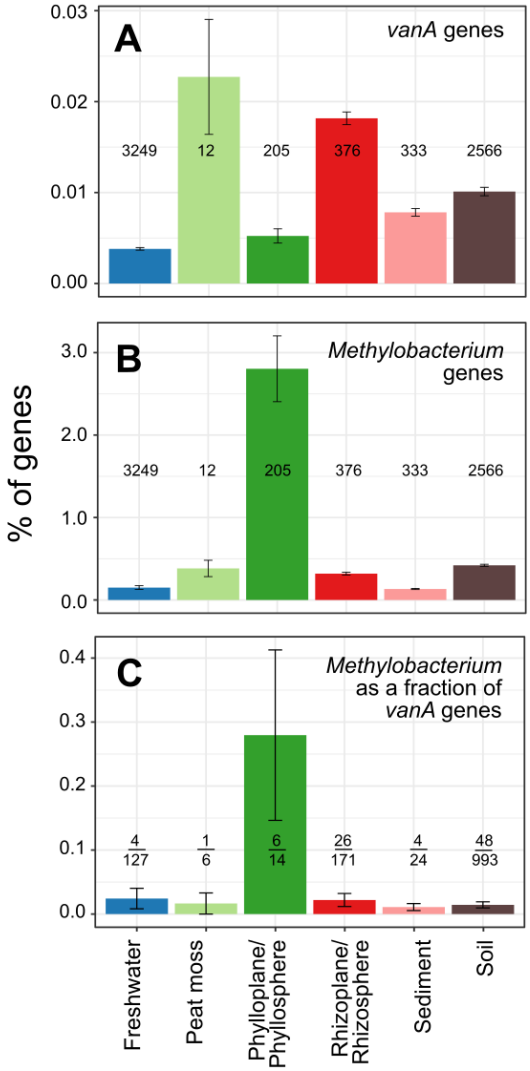

Figure 8. Among *Methylobacterium vanA* sequences in published metagenomes, the *M. nodulans* clade is most abundant.
Sequences of 182 *Methylobacterium*-associated *vanA* gene fragments found in published metagenomes were added using pplacer [47] to a phylogeny of full-length *vanA* genes sequenced from reference genomes. 166 genes that were classified by IMG as *Methylobacterium* but clustered outside of the genus are not shown. Colored dots indicate the ecosystem type from which the metagenome sample originated, with size scaled to the likelihood weight ratio of the pplacer classification as a measure of confidence in the placement. 114 genes (63%) are classified as *M. nodulans*; 31 genes (17%) as *Methylobacterium sp.* AMS5, and 37 genes (20%) as *M. aquaticum*. Inset bar plot: abundance of *Methylobacterium vanA* genes, shaded by clade, in each genome in which they were found. Each bar represents one genome (genome IDs not shown).